ELSEVIER

Journal of Alloys and Compounds 368 (2004) 326–332

Journal of ALLOYS AND COMPOUNDS

www.elsevier.com/locate/jallcom

Synthesis, structure and photoluminescence of novel lanthanide (Tb(III), Gd(III)) complexes with 6-diphenylamine carbonyl 2-pyridine carboxylate

Bao-Li An [a,b,*], Meng-Lian Gong [b,1], Kok-Wai Cheah [c], Wai-Kwok Wong [d], Ji-Ming Zhang [a]

[a] *Department of Chemistry, College of Science, Shanghai University, Shanghai 200436, China*
[b] *State Key Laboratory of Optoelectronic Materials and Technologies, Sun Yat-sen University, Guangzhou 510275, China*
[c] *Department of Physics, Hong Kong Baptist University, Hong Kong, China*
[d] *Department of Chemistry, Hong Kong Baptist University, Hong Kong, China*

Received 14 April 2003; accepted 30 July 2003

Abstract

A novel organic ligand, 6-diphenylamine carbonyl 2-pyridine carboxylic acid (HDPAP), and the corresponding lanthanide complexes, tris(6-diphenylamine carbonyl 2-pyridine carboxylato) terbium(III) (Tb-DPAP) and tris(6-diphenylamine carbonyl 2-pyridine carboxylato) gadolinium(III) (Gd-DPAP) have been designed and synthesized. The crystal structure and photoluminescence of Tb-DPAP and Gd-DPAP have been studied. The results showed that the lanthanide complexes have electroneutral structures, and the solid terbium complex emits characteristic green fluorescence of Tb(III) ions at room temperature while the gadolinium complex emits the DPAP ligand phosphorescence. The lowest triplet level of DPAP ligand was calculated from the phosphorescence spectrum of Gd-DPAP in *N*,*N*-dimethyl formamide (DMF) dilute solution determined at 77 K, and the energy transfer mechanisms in the lanthanide complexes were discussed. The lifetimes of the $^5D_4$ levels of Tb^{3+} ions in the terbium complex were examined using time-resolved spectroscopy, and the values are 0.0153 ± 0.0001 ms for solid $Tb(DPAP)_3{\cdot}11.5H_2O$ and 0.074 ± 0.007 ms for 2.5×10^{-5} mol/l Tb-DPAP ethanol solution.

Keywords: Optical materials; Chemical synthesis; Crystal structure; Luminescence; Thermal analysis

1. Introduction

Organic electroluminescence (OEL) has been studied extensively for its opportunities of low drive voltage, suitability for integrated circuit and potential application for large plate display [1,2].

As some lanthanide ions, e.g. Eu^{3+} and Tb^{3+}, possess good luminescence characteristics (high color purity) based on the transitions between the 4f energy levels, a series of compounds activated by Eu^{3+} and Tb^{3+} have been studied for practical application as phosphors and laser materials [3,4]. Terbium(III) has four narrow emission bands corresponding to the $^5D_4 \rightarrow {}^7F_j$ transitions, where $j = 6$, 5, 4, 3. The strongest transition, $^5D_4 \rightarrow {}^7F_5$, occurs at approximately 544 nm, the narrow intense green terbium luminescence [5]. Several ternary rare earth complexes have been applied to prepare OEL devices that showed weak visible emission and low electroluminescence efficiency [6–9]. In principle, electroneutral metal complexes may form uniform thin film in vacuum vapor deposition and are reasonably stable to heat, which is required for OEL displays [10]. Investigating the relationship between the structures of organic ligands and the energy levels of lanthanide ions will give evidences for designing high luminescent lanthanide organic complexes. In this paper, a novel organic ligand, 6-diphenylamine carbonyl 2-pyridine carboxylic acid (HDPAP), was designed and synthesized. The corresponding terbium and gadolinium complexes, tris(6-diphenylamine carbonyl 2-pyridine carboxylato) terbium(III) (Tb-DPAP) and tris(6-diphenylamine carbonyl 2-pyridine carboxylato) gadolinium(III) (Gd-DPAP), were synthesized, and the structure and luminescence

* Corresponding author. Tel.: +86-21-6613-2670; fax: +86-21-6613-2797.
E-mail addresses: anbaolii@263.sina.com (B.-L. An), cesgml@zsu.edu.cn (M.-L. Gong).
[1] Co-corresponding author.

0925-8388/$ – see front matter © 2003 Elsevier B.V. All rights reserved.
doi:10.1016/j.jallcom.2003.07.020

properties for the lanthanide complexes have been investigated.

2. Experimental

2.1. Preparation of 6-diphenylamine carbonyl 2-pyridine carboxylic acid

2,6-Dichlorocarbonyl pyridine (DCP) was prepared by a reaction of 2,6-pyridine dicarboxylic acid (H_2DPA) and thionyl chloride [11] with high yield of 95%. Diphenylamine (4.14 g) dissolved in dried benzene was slowly added to 5.0 g of DCP dissolved in dried benzene, and was stirred for 5 h at 50 °C. The mixture was then cooled to room temperature and filtered to remove the white precipitate. The benzene solution was concentrated in vacuum and then hydrolyzed at 40 °C for 2 h. The pH value of the solution was adjusted to 9.5 using 2.0 mol/l aqueous NaOH; the mixture was filtered and the pH value of the filtrate was adjusted to 3.0 using 2.0 mol/l HCl, giving a white precipitate. The white precipitate was recrystallized in 95% ethanol: acetone (1:1 (v:v)), giving 2.8 g of 6-diphenylamine carbonyl 2-pyridine carboxylic acid with a yield 35% and mp 74–77 °C.

The synthesis route is expressed as follows:

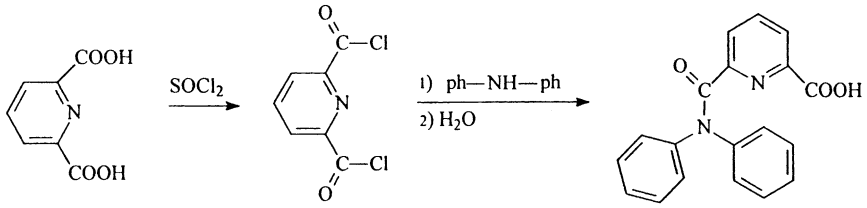

H_2DPA DCP HDPAP

2.2. Preparation of $Tb(DPAP)_3{\cdot}11.5H_2O$ and $Gd(DPAP)_3{\cdot}12H_2O$

The $Tb(DPAP)_3{\cdot}11.5H_2O$ complex was prepared by adding 12.0 mmol of HDPAP dissolved in ethanol to an aqueous solution containing 4.0 mmol $TbCl_3$, which was obtained by reaction of Tb_4O_7 (99.95%, Zhu-jiang Smeltery Co.) and HCl (6.0 mol/l). The pH value of the mixture was adjusted to 5 by adding an aqueous solution of sodium hydroxide, stirred 12 h at 40 °C. After 240 h, colorless cubic crystals were precipitated from the solution, and was filtered out and washed with deionized water and 95% ethanol. A hydrated complex $Tb(DPAP)_3{\cdot}11.5H_2O$ was obtained with a yield of 38%.

The $Gd(DPAP)_3{\cdot}12H_2O$ was prepared as the synthesis method of $Tb(DPAP)_3{\cdot}11.5H_2O$ with a yield of 62%.

2.3. Measurements and apparatus

Elemental analysis for the samples was carried out with an Elementar vario EL elemental analyzer. IR spectra in the region 4000–400 cm^{-1} were recorded on a Bruker infrared spectrophotometer using conventional KBr method. FAB-MS spectra were performed on a VG ZAB-HS spectrometer. The ^1H NMR spectra were recorded on a USA Varian UNITYINOVA-500 spectrometer (500 MHz). The excitation and emission spectra were recorded on a Aminco Bowman Series fluorescence spectrophotometer with both excitation and emission slits at 1.0, 4.0 and 8.0 nm for solid $Tb(DPAP)_3{\cdot}11.5H_2O$, Tb(DPAP) ethanol dilute solution and solid $Gd(DPAP)_3{\cdot}12H_2O$, respectively, at room temperature, and with the same PMT at 700 V. Fluorescence lifetimes were measured using an EMG 201 MSC quasi-molecular 308 nm laser by monitoring $^5D_4 \rightarrow {}^7F_5$ emission line of Tb^{3+} at room temperature. Phosphorescence spectra were recorded on SPEX 1934D phosphorescence spectrometer at 77 K, with both excitation and emission slits at 4.0 mm and with the light pulse width of 1.0 ms and pulse interval of 0.001 ms. UV spectra were recorded on a Varlan UV-Vis spectrophotometer. Thermogravimetric analysis (TGA) was carried out up to 750 °C in nitrogen atmosphere on a Netzsch TG209 thermogravimetric analyzer.

Diffraction intensities for the complexes were collected at 21 °C on a Siemens R3m diffractometer using the ω-scan technique. Lorentz-polarization and absorption corrections were applied [12]. The structures was solved with the direct method and refined with full-matrix least-squares using the SHELXS-97 and SHELXL-97 programs, respectively [13,14]. Anisotropic thermal parameters were applied to all non-hydrogen atoms, and the organic hydrogen atoms were generated geometrically (C–H 0.96 Å); the aqua hydrogen atoms were located from difference maps and refined with isotropic temperature factors. Analytical expressions of neutral-atom scattering factors were employed, and anomalous dispersion corrections were incorporated [15]. Crystal data as well as details of data collection and refinement for the complex are summarized in Table 1. Selected bond distances and bond angles for $Tb(DPAP)_3{\cdot}11.5H_2O$ and $Gd(DPAP)_3{\cdot}12H_2O$ are listed in Tables 2 and 3, respectively. Drawings were produced with SHELXTL [16].

3. Results and discussion

3.1. Elemental analysis and IR absorption

The elemental analysis data for $C_{19}H_{14}N_2O_3$ (HDPAP) are: found (calcd.) C 71.48 (71.69), H 4.43 (4.43), and N

Table 1
Crystallographic data for complexes $Tb(DPAP)_3 \cdot 11.5H_2O$ and $Gd(DPAP)_3 \cdot 12H_2O$

Complexes	Tb-DPAP	Gd-DPAP
Formula	$C_{57}H_{62}N_6O_{20.5}Tb$	$C_{57}H_{63}GdN_6O_{21}$
Formula weight	1318.05	1325.37
Crystal system	Cubic	Cubic
Volume (Å^3)	12419(9)	12025.5(9)
Density (calculated) (g cm^{-3})	1.410	1.437
Space group	$Pa\bar{3}$	$Pa\bar{3}$
Unit cell dimensions	$a = b = c = 23.158\ (10)$ Å $\alpha = \beta = \gamma = 90^\circ$	$a = b = c = 22.9105(10)$ Å $\alpha = \beta = \gamma = 90^\circ$
Z	8	8
$F(0\,0\,0)$	5400	5240
Scan type	ω	ω
θ range/for data collection (°)	2.15–27.03	1.54–27.50
Reflection collected	7636	67544
Independent reflections	4162 ($R_{int} = 0.0791$)	4606 ($R_{int} = 0.0466$)
Radiation λ (Mo Kα) (Å)	0.71073	0.71073
Absorption coefficient μ (mm^{-1})	1.216	1.183
Goodness-of-fit on F^2	0.978	1.083
Data/restraints/parameters	4162/0/256	4606/0/257
Final R indices ($I \geq 2\sigma(1)$)	$R_1 = 0.0630$ $\omega R_2 = 0.1428$	$R_1 = 0.0347$ ωR_2=0.0978
Largest difference peak and hole	0.814 and −0.626 eÅ^{-3}	0.698 and −0.573 eA^{-3}

Table 2
Some bond lengths (Å) and angles (°) for complex Tb-DPAP

Tb(1)–O(2)	2.381(5)	Tb(1)–O(3)	2.453(5)
Tb(1)–N(1)	2.577(6)	O(2)–C(1)	1.282(9)
O(1)–C(1)	1.274(9)	O(3)–C(7)	1.255(8)
O(2)–Tb(1)–O(2)#2	79.85(19)	O(2)–Tb(1)–O(3)# 1	89.39(17)
O(2)–Tb(1)–O(3)#2	148.78(16)	O(3)#2–Tb(1)–O(3)	73.93(19)
O(2)–Tb(1)–O(3)	127.24(17)	O(2)–Tb(1)–N(1)# 1	82.45(17)
O(2)–Tb(1)–N(1)#2	142.77(19)	O(3)–Tb(1)–N(1)# 1	127.05(17)
O(3)–Tb(1)–N(1)#2	66.50(16)	O(2)#1–Tb(1)–N(1)	142.77(19)
O(2)–Tb(1)–N(1)	64.89(18)	O(2)#2–Tb(1)–N(1)	82.45(17)
O(3)#2–Tb(1)–N(1)	127.05(17)	O(3)#l–Tb(1)–N(1)	66.50(16)
O(3)–Tb(1)–N(1)	62.52(17)	N(1)#1–Tb(1)–N(1)	118.60(5)
C(1)–O(2)–Tb(1)	125.2(5)	C(7)–O(3)–Tb(1)	126.7(5)
C(6)–N(1)–Th(1)	120.2(4)	C(2)–N(1)–Th(1)	115.0(4)

Symmetry transformations used to generate equivalent atoms: #1—*y*, *z*, *x*; #2—*z*, *x*, *y*.

Table 3
Some bond lengths (Å) and angles (°) for Gd-DPAP

Gd(1)–O(3)	2.428(2)	Gd(1)–O(2)	2.368(3)
Gd(1)–N(1)	2.558(3)	O(1)–C(1)	1.231(5)
O(2)–C(1)	1.269(5)	O(3)–C(7)	1.242(4)
O(2)#1–Gd(1)–O(2)	79.59(11)	O(2)–Gd(1)–O(3)	126.72(9)
O(2)#1–Gd(1)–O(3)	149.46(9)	O(3)–Gd(1)–N(1)#1	126.99(9)
O(3)–Od(1)–O(3)#1	74.05(10)	O(2)–Gd(1)–O(3)#1	89.62(10)
O(3)–Gd(1)–N(1)#2	66.67(9)	O(2)–Gd(1)–N(1)#1	82.93(9)
O(2)–Gd(1)–N(1)#2	142.59(10)	O(3)–Gd(1)–N(1)	62.13(9)
N(1)#2–Od(1)–N(1)	118.55(3)	O(2)–Od(1)–N(1)	64.80(9)
C(1)–O(2)–Od(1)	126.0(2)	C(7)–O(3)–Gd(1)	126.7(2)
C(2)–N(1)–Od(1)	115.4(2)	C(6)–N(1)–Gd(1)	120.8(2)

8.89 (8.80). IR (KBr) ν_{max} 3238.2, 3078.0, 1754.8, 1653.2, 1591.4, 1489.8, 1373.6, 756.5 and 695.5 cm^{-1}. ^{1}H NMR in CD_3SOCD_3: 13.084(1H, s), 7.921(1H, t, $^3J = 7.5$ Hz), 7.893 (1H, d, d, $^3J = 8.0$ Hz, $^4J = 2.0$ Hz), 7.768 (d, d, $^3J = 7.25$ Hz, $^4J = 1.75$ Hz), 7.284 (8H, s) and 7.204 (2H, s). FAB-MS: *m*/*z* 319 ($[M + H]^+$).

The complexes were verified by elemental analysis, IR spectroscopy and X-ray crystal analysis.

The elemental analysis results for Tb-DPAP are: found (calcd. for $TbC_{57}H_{62}N_6O_{20.5}$) C 51.86 (51.94), H 4.83 (4.74), N 6.36 (6.39) and Tb 12.67 (12.06). IR (KBr) ν_{max} 3418.7, 3109.8, 3070.2, 1619.8, 1567.7, 1490.4, 1376.4, 1269.8, 757.0 and 699.9 cm^{-1}. The elemental analysis results for Gd-DPAP are: found (calcd. for $GdC_{57}H_{63}N_6O_{21}$) C 51.52 (51.65), H 4.52 (4.79), N 6.10 (6.34), Gd 12.31 (11.86). IR (KBr) ν_{max} 3423.5, 3105.0, 3064.3, 1620.3, 1568.9, 1490.9, 1375.6, 1270.9, 699.8 cm^{-1}.

3.2. Crystal structure

The crystal structure of $Tb(DPAP)_3 \cdot 11.5H_2O$ consists of the mononuclear $Tb(DPAP)_3$ molecules and lattice water molecules. As shown in Fig. 1, the Tb(III) atom is coordinated in a tri-capped trigonal prism geometry with three nitrogen atoms [Tb(1)–N(1) 2.577(6) Å] in pyridine ring, three carboxylate oxygen atoms [Tb(1)–O(2) 2.381(5) Å; O(2)–Tb(1)–N(1) 64.9(2)°] and three carbonyl oxygen atoms [Tb(1)–O(3) 2.453(5) Å, O(3)–Tb(1)–N(1) 62.5(2)°] from three different DPAP ligands. The coordination number of central Tb(III) atom here is 9, reaching its saturated

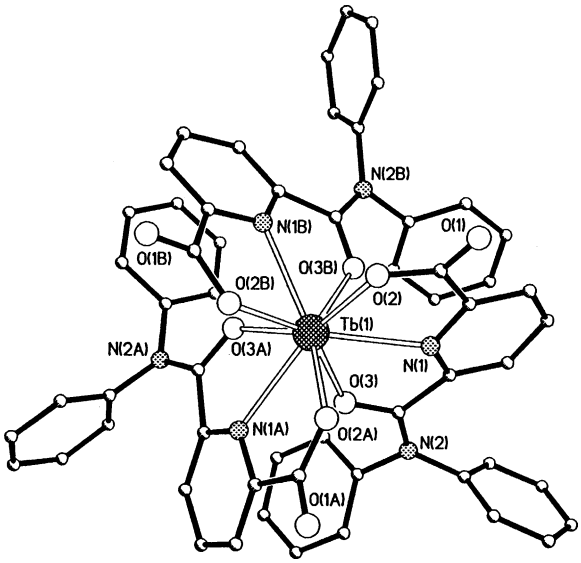

Fig. 1. Crystal structure of $Tb(DPAP)_3{\cdot}11.5H_2O$.

state, therefore, the lattice water molecules only form donor hydrogen bonds [O(1w) · · · O 2.77(1)–2.98(2) Å] with the carboxylate oxygen atoms. Thus, compared with the ternary terbium-β-diketonato-base complexes [5,17], where the coordination numbers are 6 or 8, the mononuclear $Tb(DPAP)_3$ molecules in this structure would have better chemical thermodynamic stability.

The crystal structure of $Gd(DPAP)_3{\cdot}12H_2O$ is similar to that of $Tb(DPAP)_3{\cdot}11.5H_2O$, and a little differences of the bond lengths and bond angles between the two complexes have been observed. The Gd(III) atom is coordinated in a tri-capped trigonal prism geometry with three nitrogen atoms [Gd(1)–N(1) 2.558(3) Å] in pyridine ring, three carboxylate oxygen atoms [Gd(1)–O(2) 2.368(3) Å; O(2)–Gd(1)–N(1) 64.80(9)°] and three carbonyl oxygen atoms [Gd(1)–O(3) 2.428(2) Å, O(3)–Gd(1)–N(1) 62.13(9)°] from three different DPAP ligands.

3.3. UV absorption spectra

UV absorption spectra for 2.5×10^{-5} mol/l HDPAP, 1.0×10^{-5} mol/l $Tb(DPAP)_3$ and 1.0×10^{-5} mol/l $Gd(DPAP)_3$ ethanol solutions were determined at same conditions, the maximum absorption wavelengths and molecular absorption coefficients are given in Table 4. The absorption bands for $Tb(DPAP)_3$ and $Gd(DPAP)_3$ dilute solutions shifted to longer wavelengths compared with that of HDPAP ligand, which was attributed to the metal coordination.

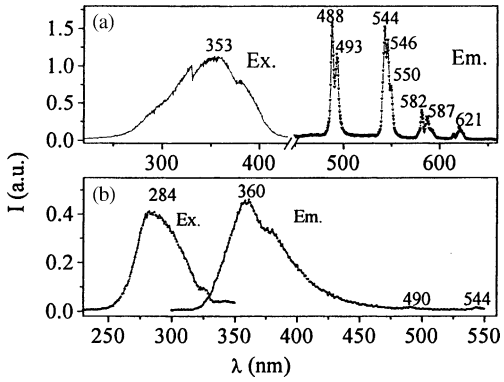

Fig. 2. Excitation and emission spectra for (a) solid $Tb(DPAP)_3{\cdot}11.5H_2O$ and (b) $1.0{\times}10^{-4}$ mol/l $Tb(DPAP)_3$ ethanol solution.

3.4. Excitation and emission spectra

The excitation spectra for the original $Tb(DPAP)_3{\cdot}11.5H_2O$ complex and 1.0×10^{-4} mol/l $Tb(DPAP)_3$ ethanol solution are shown in Fig. 2, monitored at 544 and 361 nm, respectively. The 300–400 nm wide band centered at 353 nm was observed on the excitation spectrum for the solid $Tb(DPAP)_3{\cdot}11.5H_2O$ complex.

The emission spectrum of solid Tb-DPAP complex consists of four main lines at 488 nm ($^5D_4 \rightarrow {}^7F_6$), 544 nm ($^5D_4 \rightarrow {}^7F_5$), 582 nm ($^5D_4 \rightarrow {}^7F_4$) and 621 nm ($^5D_4 \rightarrow {}^7F_3$) (Fig. 2(a)). The $^5D_4 \rightarrow {}^7F_6$, $^5D_4 \rightarrow {}^7F_5$ and $^5D_4 \rightarrow {}^7F_4$ emission bands split into two peaks (488 and 493 nm), three peaks (544, 546 and 550 nm) and two peaks (582 and 587 nm), respectively, which was attributed to the crystal field splitting. The emission band ($^5D_4 \rightarrow {}^7F_5$) is obviously stronger than the emission band ($^5D_4 \rightarrow {}^7F_6$) for terbium-β-diketone chelates [5,17], but the emission at 488 nm is a little stronger than that at 544 nm for solid $Tb(DPAP)_3{\cdot}11.5H_2O$ complex. The reason was attributed

Table 4
The photophysical properties of $Tb(DPAP)_3$ and $Gd(DPAP)_3$ complexes

Sample	UV absorption		Fluorescence			Lifetimes
	λ_{max} (nm)	ε ($\times 10^{-4}$)[a]	λ_{ex} (nm)	λ_{em} (nm)	I (a.u.)	τ (ms)
2.5×10^{-5} mol/l HDPAP	277	1.4				
1.0×10^{-4} mol/l $Tb(DPAP)_3$	293	2.84[b]	284	360	0.457	0.074 ± 0.007[c]
1.0×10^{-5} mol/l $Gd(DPAP)_3$	293	2.84				
$Tb(DPAP)_3{\cdot}11.5H_2O$			353	544	1.50	0.0153 ± 0.0001
$Gd(DPAP)_3{\cdot}12H_2O$			351	493	3.91	

[a] The unit of ε is $mol^{-1}\,dm^3\,cm^{-1}$.
[b] The UV spectrum for 1.0×10^{-5} mol/l $Tb(DPAP)_3$ ethanol solution was determined.
[c] The first decay lifetime is 0.074 ± 0.007 ms, and the second decay lifetime is 0.30 ± 0.03 ms.

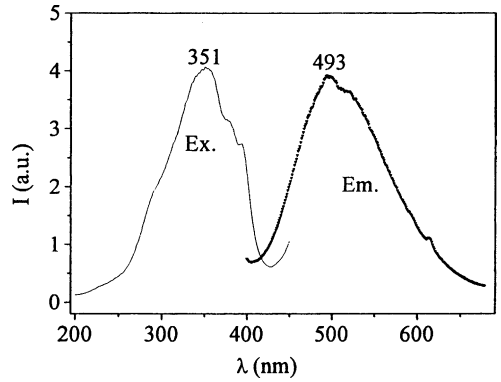

Fig. 3. Excitation and emission spectra for solid $Gd(DPAP)_3{\cdot}12H_2O$ complex.

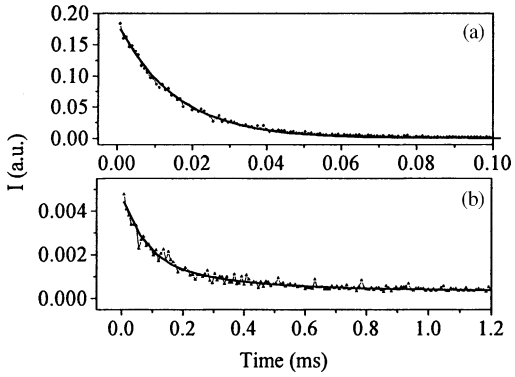

Fig. 4. The time-resolved spectra for (a) original $Tb(DPAP)_3{\cdot}11.5H_2O$ and (b) 2.5×10^{-5} mol/l $Tb(DPAP)_3$ ethanol solution. The line curves are the first-order exponential decay fit curve and the second-order exponential decay fit curve for the former and the latter, respectively, and the symbol line are the lifetime decay curves.

to that the emission ($^5D_4 \rightarrow {}^7F_6$) is an electric dipole transition, which is considerably affected by the ligand field while the $^5D_4 \rightarrow {}^7F_5$ emission is a magnetic dipole transition, which is less affected by the ligand field. Week Tb^{3+} ions emission peaks and strong broad DPAP ligand fluorescence emission band centered at 361 nm were observed on the emission spectrum for 1.0×10^{-4} mol/l $Tb(DPAP)_3$ ethanol solution at room temperature (Fig. 2(b)).

The excitation and emission spectra for the original $Gd(DPAP)_3{\cdot}12H_2O$ is shown in Fig. 3. A broad excitation band (300–400 nm) centered at 351 nm was observed on the excitation spectrum for solid $Gd(DPAP)_3{\cdot}12H_2O$, and the emission spectrum for the solid gadolinium complex showed a wide phosphorescence emission band centered at 493 nm at room temperature, which was attributed to the DPAP ligand emission. Due to the temperature quenching effect, the DPAP ligand phosphorescence emission was not observed for 1.0×10^{-4} mol/l $Gd(DPAP)_3$ ethanol solution at room temperature.

3.5. Lifetimes

The lifetimes of $^5D_4$ excited state of Tb^{3+} for solid $Tb(DPAP)_3{\cdot}11.5H_2O$ and 2.5×10^{-5} mol/l $Tb(DPAP)_3$ ethanol solution were measured by time-resolved spectroscopy at room temperature (Fig. 4). The lifetime value for the solid complex was calculated through the first-order exponential decay method [18], and the result was shown in Table 4. The lifetime curve for the latter was fitted to be very suitable for the second-order exponential decay curve, and the decay equation was

$$I = 0.00035 + 0.0029e^{-(t/0.074)} + 0.0015e^{-(t/0.30)}$$

where "I" is the relative intensity of fluorescence, and "t" is the decay time. The results indicated that the decay mechanism of $^5D_4$ excited state of Tb^{3+} for $Tb(DPAP)_3$ ethanol dilute solution might be different from that for solid $Tb(DPAP)_3{\cdot}11.5H_2O$.

3.6. Triplet state of the ligand and energy transfer

The value of the lowest triplet state for HDPAP ligand is 20477 cm^{-1}, calculated from the phosphorescence spectrum for $Gd(DPAP)_3$ complex dimethyl formamide (DMF) dilute solution determined at 77 K (Fig. 5). The excitation and emission bands for $Gd(DPAP)_3$–DMF dilute solution shifted to shorter wavelengths compared with those for solid Gd(DPAP) complex, and the phosphorescence emission band of the former was evidently broader than that of the latter. The triplet state of the DPAP ligand was only higher by 23 cm^{-1} than the lowest excited state of Tb^{3+}, $^5D_4$, not matched with the lowest excited state of Tb^{3+} [19,20]. However, strong characteristic emissions of Tb^{3+} ions for the solid terbium complex were observed, which was attributed to the following factors. First, the symmetry alteration of the Tb^{3+} ions in the complex might be beneficial to the energy transfer in the solid terbium complex; second, the good rigid planar structure of the terbium complex was formed by the three tridentate DPAP ligands, which sensitized the luminescence [19]; third, the lengths of Tb(1)–O(2) were shorter than those of Tb(1)–O(3), and the decrease of distances between the central Tb^{3+} ions and donor oxygen

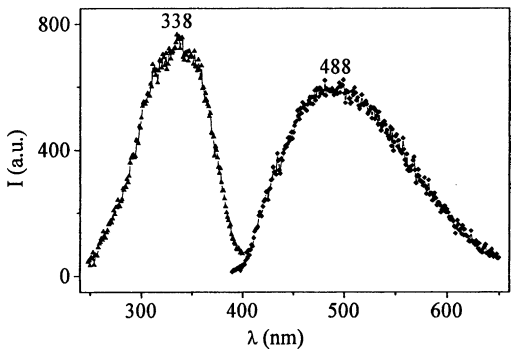

Fig. 5. Excitation (▲) and phosphorescence (◆) spectra for $Gd(DPAP)_3$–DMF solution at 77 K.

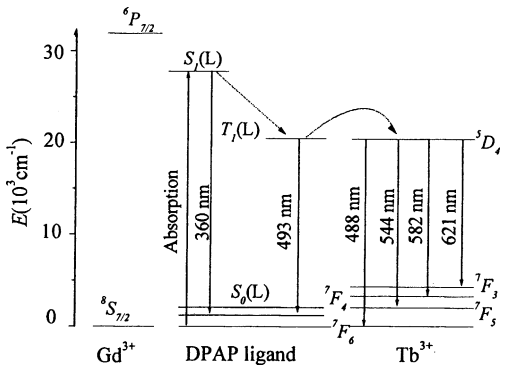

Fig. 6. Energy transfer scheme for $Tb(DPAP)_3$ and $Gd(DPAP)_3$ complexes.

atoms from the carboxylate groups was beneficial to the energy transfer from the ligands to the central ions.

The excitation spectrum for solid $Tb(DPAP)_3$ complex showed that most of the excitation energy was mainly absorbed by the ligand, and then transferred to the central Tb^{3+} ion, then the characteristic fluorescence of the latter emitted. The dominant luminescence mechanism for the solid $Tb(DPAP)_3$ complex was given as luminescence from the triplet state of the ligand to the central terbium ion ($L^* \rightarrow M$) (shown in Fig. 6).

The DPAP ligand fluorescence with week characteristic emission of Tb^{3+} ions was observed on the emission spectrum for the $Tb(DPAP)_3$ ethanol dilute solution at room temperature, due to the thermal deactivation process since the energy gap between the excited triplet energy levels of the DPAP ligands [T^*(L)] and the lowest excited energy levels of Tb^{3+} ($^5D_4$) was small [20].

The solid gadolinium complex emitted the phosphorescence emission of DPAP ligands, not emitted characteristic emission of Gd^{3+} ions, which was attributed to that the lowest triplet energy levels of the DPAP ligands were lower than those of the lowest excited state levels of Gd^{3+} ions, and the energy could not be transferred from the triplet energy levels of the DPAP ligands to the gadolinium ions (Fig. 6).

3.7. Thermal stability

The temperature dependence of weight loss of the original $Tb(DPAP)_3{\cdot}11.5H_2O$ is shown in Fig. 7. The initial weight loss of $Tb(DPAP)_3{\cdot}11.5H_2O$ started at about 20 °C is due to the water loss. The second stage in region of 325–750 °C is attributed to elimination and/or decomposition of DPAP ligands. The results showed that $Tb(DPAP)_3$ complex has good thermal stability.

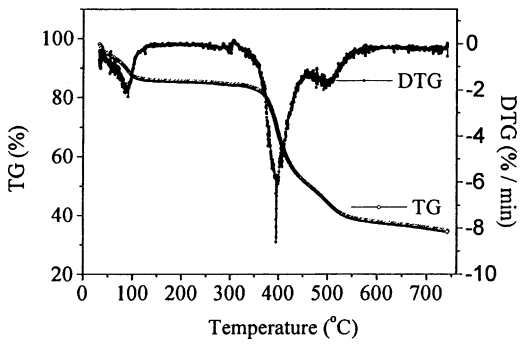

Fig. 7. TG and DTG curves for original $Tb(DPAP)_3{\cdot}11.5H_2O$.

4. Conclusions

A novel terbium(III) complex and a novel gadolinium(III) complex, tris(diphenylamine carbonyl 2-pyridine carboxylato) terbium(III) and tris(diphenylamine carbonyl 2-pyridine carboxylato) gadolinium(III), have been synthesized. The crystal structures of the terbium complex and the gadolinium complex showed that they are electroneutral molecules, in which the central Tb^{3+} and Gd^{3+} ions are wrapped by three novel tridentate organic ligands, with some water molecules located around the outer shell of the complexes. The solid terbium complex emits characteristic emission of Tb^{3+} ions, and the lifetime of the $^5D_4$ excited states of Tb^{3+} ions in solid $Tb(DAPA)_3{\cdot}11.5H_2O$ is 0.0153 ± 0.0001 ms. The terbium complex has good thermal stability. The energy gap between the excited triplet energy levels of the organic ligands [T^*(L)] and the lowest excited energy levels of rare earth ions is important factor to the luminescence of rare earth organic complexes.

Acknowledgements

Supported by a grant from the Scientific and technical project of Guangdong province (B10502), a grant from the State Key Laboratory of Optoelectronic Materials and Technologies (2000), and also supported by a grant from adolescent fund of Shanghai Municipal Education Committee (03AQ95).

References

[1] P.K.H. Ho, D.S. Thomas, R.H. Friend, N. Tessler, Science 285 (1999) 233.
[2] R.H. Friend, R.W. Gymer, A.B. Homes, J.H. Buroughes, R.N. Marks, C. Taliani, D.D.C. Bradley, D.A. Dos Santos, J.L. Brédas, M. Lögdlund, W.R. Salaneck, Nature 397 (1999) 121.
[3] G.N. Wan den Hoven, E. Snoeks, A. Polman, J.W.M. van Uffelen, Y.S. Oci, M.K. Smit, Appl. Phys. Lett. 62 (1993) 3065.
[4] C.K. Ryu, H. Choi, K. Kim, Appl. Phys. Lett. 66 (1996) 2496.
[5] N. Filipescu, W.F. Sager, F.A. Serafin, J. Phys. Chem. 68 (1964) 3324.
[6] Y. Kawamura, Y. Wada, Y. Hasegawa, M. Iwamuro, T. Kitamura, S. Yanagida, Appl. Phys. Lett. 74 (1999) 3245.
[7] D. Zhao, Z. Hong, C. Liang, D. Zhao, X. Liu, W. Li, C.S. Lee, S.T. Lee, Thin Solid Films 363 (2000) 208.
[8] C.J. Liang, D. Zhao, Z.R. Hong, D.X. Zhao, X.Y. Liu, W.L. Li, J.B. Peng, J.Q. Yu, C.S. Lee, S.T. Lee, Appl. Phys. Lett. 76 (2000) 67.

[9] X.C. Gao, H. Cao, C. Huang, B. Li, S. Umitani, Appl. Phys. Lett. 72 (1998) 2217.
[10] T. Sano, Y. Nishio, Y. Hamada, H. Takahashi, T. Usuki, K. Shibata, J. Mater. Chem. 10 (2000) 157.
[11] B.L. An, X. Shi, W.K. Wong, K.W. Cheah, R.H. Li, Y.S. Yang, M.L. Gong, J. Luminesc. 99 (2002) 155.
[12] A.C.T. North, D.C. Phillips, F.S. Mathews, Acta Crystallogr. Sect. A 24 (1968) 351.
[13] G.M. Sheldrick, SHELXS-97, Program for Crystal Structure Solution, Göttingen University, Göttingen, Germany, 1997.
[14] G.M. Sheldrick, SHELXL-97, Program for Crystal Structure Refinement, Göttingen University, Göttingen, Germany, 1997.
[15] D.T. Cromer, Intemational Table for X-Ray Crystallography, vol. C (Tables 4.2.6.8 and 6.1.1.4), Kluwer Academic Publisher, Dordrecht, 1992.
[16] G.M. Sheldrick, SHELXTL, Version 5, Siemens Industrial Automation Inc., Madison, WI, USA, 1995.
[17] Q. Li, J.D. Zhou, C.H. Huang, G.Q. Yao, Y.F. Zhou, G.Z.F. Mei, J.Z.H. Song, Acta Chim. Sin. 56 (1998) 52 (in Chinese).
[18] G.Z. Chen, X.Z. Huang, Z.Z. Zheng, J.G. Xu, Z.B. Wang, Fluorescence Analysis Methods, Science Press, Peking, 1990 (in Chinese).
[19] Y.S. Yang, M.L. Gong, Y.Y. Li, H.Y. Lei, S.L. Wu, J. Alloys Comp. 207–208 (1994) 112.
[20] S. Sato, M. Wada, Bull. Chem. Soc. Jpn. 43 (1970) 1955.